Journal of Civil Engineering and Urban Planning (2026)
Clausius Scientific Press, Canada

DOI: 10.23977/jceup.2026.080105
ISSN 2616-3969 Vol. 8 Num. 1

Study on Remaining Bearing Capacity of Local Corrosion Circular Concrete Filled Steel Tube Column after Impact

Shaokun Zhou

Key Laboratory of Urban Security and Disaster Engineering of Ministry of Education, Beijing University of Technology, Beijing, 100124, China

Keywords: Concrete Filled Steel Tube Column; Local Corrosion; Residual Load-Bearing Capacity

Abstract: Concrete filled steel tube (CFST) columns are widely used in bridge and other engineering structures due to their excellent mechanical properties and construction convenience. However, during long-term service, the anti-corrosion coating on the steel tube surface may fail due to environmental erosion, leading to localized corrosion, which subsequently compromises structural safety. Additionally, accidental loads such as vehicle impacts can also cause structural damage. Currently, there is limited research on the residual bearing capacity of locally corroded CFST columns after impact loading. In this paper, a finite element model of circular CFST columns with localized corrosion after impact was established using ABAQUS software. The effects of steel strength, concrete strength, circumferential corrosion angle, axial corrosion length, corrosion depth ratio, and impact energy on the residual bearing capacity were systematically analyzed. The results indicate that increasing steel and concrete strength enhances the residual bearing capacity; larger circumferential corrosion angles and corrosion depth ratios significantly reduce the residual bearing capacity; the axial corrosion length has no significant effect on the residual bearing capacity; and higher impact energy leads to greater structural damage and lower residual bearing capacity. The findings provide theoretical references for damage assessment and reinforcement design of locally corroded CFST columns.

1. Introduction

Concrete filled steel tube (CFST) refers to structural components where steel tubes are filled with concrete, with both the steel tubes and core concrete jointly bearing external loads. Conventional CFST sections come in circular, square, rectangular, polygonal, rounded-end, and elliptical shapes, with circular and square cross-sections being the most widely used in engineering applications. The hoop restraint effect of steel tubes on core concrete subjects the structure to triaxial compressive stress under axial compression conditions. This stress distribution significantly delays the development of longitudinal cracks in core concrete after compression, thereby substantially enhancing its compressive strength and ductility. Simultaneously, the core concrete's filling support effectively suppresses local buckling deformation of steel tube walls, further improving the overall stiffness and ultimate load-bearing capacity of CFST columns [1]. Additionally, steel tubes serve as construction formwork, facilitating concrete pouring and accelerating construction processes to significantly

shorten project timelines. Consequently, CFST columns are extensively utilized in high-rise buildings, airport structures, pedestrian bridges, and large-span bridges.

In highway bridges and urban pedestrian bridges, steel tube concrete structures have become widely adopted as vertical load-bearing piers due to their lightweight self-weight, high load-bearing capacity, superior seismic performance, and construction convenience. These concrete-filled steel tube piers effectively meet engineering requirements for bridges with varying spans and load levels, enhancing structural stability while significantly reducing construction costs, making them one of the most valuable structural solutions in bridge engineering. However, during their extended service life, these piers endure complex environmental conditions. They must withstand repeated vehicle and pedestrian loads while enduring dual exposure to natural elements and industrial pollutants. Insufficient corrosion prevention planning during design, improper application of protective coatings during construction, and inadequate maintenance of anti-corrosion measures during operation can lead to surface degradation such as coating aging, cracking, and peeling [2], exposing steel tube sections to atmospheric conditions. Corrosive agents including oxygen, moisture, chloride ions in coastal environments, and acidic gases from industrial zones may penetrate these surfaces, triggering electrochemical or chemical corrosion reactions that inevitably cause structural damage in steel tube concrete piers.

With the continuous improvement of China's transportation network and the constant increase in urban road mileage, bridges-serving as the primary load-bearing and force-transmitting components of highway infrastructure-face heightened risks of structural damage and chain safety incidents when subjected to vehicle impacts. Currently, China's motor vehicle fleet has reached 470 million units, with heavy-duty trucks and large cargo vehicles experiencing annual growth. Coupled with increasing traffic volumes and frequent adverse weather conditions, vehicle collisions with bridge piers have become increasingly common, posing severe challenges for prevention and control. Multiple high-profile accidents in recent years have highlighted the severity and complexity of this issue. Regarding research on steel-concrete composite columns, Hou Chuanchuan [3] conducted performance studies on circular steel-concrete composite components under low-level impacts, analyzing failure modes, stress states, strain conditions, and cross-sectional flexural capacity of such structures, while proposing a dynamic flexural strength formula. Lai[4] and colleagues investigated the impact resistance of UHPC externally reinforced concrete-filled steel tube (UECC) columns. Fu Chaojiang [5,6], Wang Yifan [7] and others conducted research on the axial mechanical properties of steel tube concrete columns subjected to impact.

Current research primarily focuses on the dynamic response processes of steel tube concrete columns under impact and the residual load-bearing capacity of uncorroded steel tube concrete columns, with relatively limited studies on the residual load-bearing capacity of steel tube concrete columns after localized corrosion. Therefore, this study employs numerical simulation to investigate the impact of localized corrosion on the compressive mechanical properties of circular steel tube concrete columns following impact. The effects of corrosion circumferential angle, corrosion length, impact energy, axial compression ratio, steel strength, and concrete strength are systematically analyzed.

2. Establishment of Finite Element Model

This chapter establishes a finite element model for steel tube concrete columns using ABAQUS software. Given that the impact process involves instantaneous dynamics, the ABAQUS/Explicit dynamic display module is employed for computational analysis. Steel, concrete, end plates, and stiffening ribs are modeled using three-dimensional solid elements with eight-node reduced integration formats. During impact events, the falling hammer exhibits minimal deformation,

allowing simplification into a rigid body model with shell element simulation. The five-stage stress-strain model serves as the constitutive model for low-carbon steel. Considering that the yield strength and ultimate strength of steel are influenced by strain rate variations during impacts, the Cowper-Symonds model is adopted for calculations, as demonstrated in Equation 1:

$$f_y^{\mathrm{d}}/f_y=1+(\dot{\varepsilon}/D)^{1/p} \tag{1}$$

Here, f_y^{d} represents the yield strength of steel at $\dot{\varepsilon}$, and f_y denotes the yield strength of steel. It is assumed that the strain rate effect does not vary with material hardening. The values of D and p are set to 6844s^{-1} and 3.91, respectively.

The concrete simulation employs the plastic damage model provided by ABAQUS software. The uniaxial compressive stress-strain relationship of the material adopts the model proposed by Hou [3], which incorporates constraint effect coefficients to account for the influence of external constraints from steel tube concrete on the concrete stress-strain curve. Under dynamic loading conditions, concrete also exhibits significant strain rate effects, necessitating consideration of their impact on the stress-strain curve. In this study, Equation (2) is utilized to calculate the compressive strain rate effect of concrete:

$$\sigma_d/\sigma_s=\begin{cases}(\dot{\varepsilon}_d/\dot{\varepsilon}_s)^{1.026\alpha}, \dot{\varepsilon}_d\leq 30s^{-1}\\ \gamma(\dot{\varepsilon}_d/\dot{\varepsilon}_s)^{1/3}, \dot{\varepsilon}_d>30s^{-1}\end{cases} \tag{2}$$

Where σ_d denotes the compressive strength of concrete under dynamic loading, σ_s represents the compressive strength under static loading, $\dot{\varepsilon}_d$ indicates the strain rate value during dynamic loading, and $\dot{\varepsilon}_s$ denotes the strain rate value under static loading (set to -30×10^{-6}s^{-1}), with the negative sign indicating a compressive load state. Parameters α and γ are specified in the CEB-FIP code.

When considering the tensile strain rate effect of concrete, Equation (3) is used for calculation:

$$f_{\mathrm{td}}/f_{\mathrm{ts}}=\begin{cases}(\dot{\varepsilon}_{\mathrm{d}}/\dot{\varepsilon}_{\mathrm{s}})^{\delta} & \dot{\varepsilon}_{\mathrm{d}}\leq 1s^{-1}\\ \beta(\dot{\varepsilon}_{\mathrm{d}}/\dot{\varepsilon}_{\mathrm{s}})^{1/3} & \dot{\varepsilon}_{\mathrm{d}}>1s^{-1}\end{cases} \tag{3}$$

In the formula, f_{td} represents the tensile strength of concrete under dynamic loading, f_{ts} denotes the tensile strength of concrete under static loading, $\dot{\varepsilon}_{\mathrm{d}}$ indicates the strain rate value under dynamic loading, and $\dot{\varepsilon}_{\mathrm{s}}$ represents the strain rate value under static loading, typically set to $1\times10^{-6}\mathrm{s}^{-1}$. The values for parameters δ and β are referenced from the literature by Malvar and Ross (1998).

To accurately simulate real-world experimental conditions, the model employs "Tie" connections between steel pipes and end plates, steel pipes and stiffening ribs, as well as stiffening ribs and end plates, assuming no deformation occurs at all welding joints. Surface-to-surface contacts are established between steel pipes and concrete, as well as steel pipes and impact hammers, with contact properties set to "hard contact." The Coulomb friction coefficient between steel pipes and concrete is configured at 0.6, while frictionless contact is applied between steel pipes and impact hammers. The steel-concrete composite columns are constrained with one fixed-end boundary, one simply supported boundary, or both simply supported boundaries. Finite element simulations for impact on locally corroded steel-concrete composite columns were conducted using Abaqus/Explicit dynamic analysis module. Material constitutive models incorporating strain rate effects were employed. Initial velocities were applied to impact hammers in the prestress field of the load module to simulate contact impact velocities during hammer impact on specimens. A restart output request was executed to save impact simulation results for locally corroded steel-concrete composite columns into the *Restart file.

The internal forces of locally corroded steel tube concrete columns after impact are used as the initial stress state for compression simulation. The impact analysis results obtained for these columns are imported into the Abaqus/Explicit dynamic analysis module as the initial state for compression

finite element modeling. The internal forces are released by removing end restraints, followed by reapplication of constraints. Compression simulation is conducted using the model established in the previous step as the initial state, with vertical displacements applied at the hinged ends of the columns until severe deformation occurs. Data extraction and analysis are performed based on the finite element simulation results.

3. Parameter design and analysis

3.1 Parameter design

The design parameters of the finite element model used in this study are illustrated in Figure 1, specimen net length L=1600mm, specimen diameter D=140mm, steel pipe thickness t=4.5mm, corrosion depth d=2.25mm, corrosion length l=160mm, distance h=800mm from corrosion onset to bottom surface, α representing the circumferential angle of steel pipe corrosion, and impact energy of 3.85kJ.

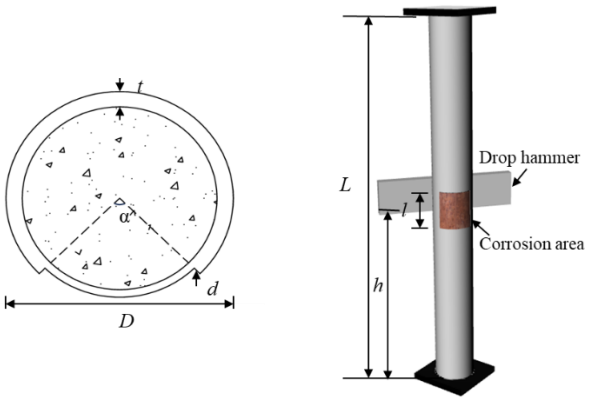

Figure 1: Schematic diagram of locally corroded steel tube concrete column

3.2 Parameter analysis

3.2.1 Steel Strength

The study selected steel yield strengths of 235MPa, 420MPa, and 690MPa as variable parameters, with other material parameters kept constant. The original bearing capacity refers to the load-bearing capacity of locally corroded steel-concrete composite columns under unimpact compression conditions, while the residual bearing capacity represents the load-bearing capacity obtained after impact compression tests. The residual bearing capacity coefficient kr is defined as the ratio of residual bearing capacity to original bearing capacity. As shown in Figure 2, both original and residual bearing capacities progressively increase with rising steel strength grades. For Q235 steel, the original bearing capacity and residual bearing capacity are 1304kN and 1023kN respectively, with a residual bearing capacity coefficient kr=0.79; for Q420 steel, these values are 1706kN and 1268kN, yielding kr=0.74; while Q690 steel demonstrates kr=0.81 for original and residual bearing capacities. Analysis reveals that steel strength grades exhibit a slight weakening effect on post-impact residual bearing capacity from Q235 to Q420, followed by a marginal enhancement effect from Q420 to Q690.

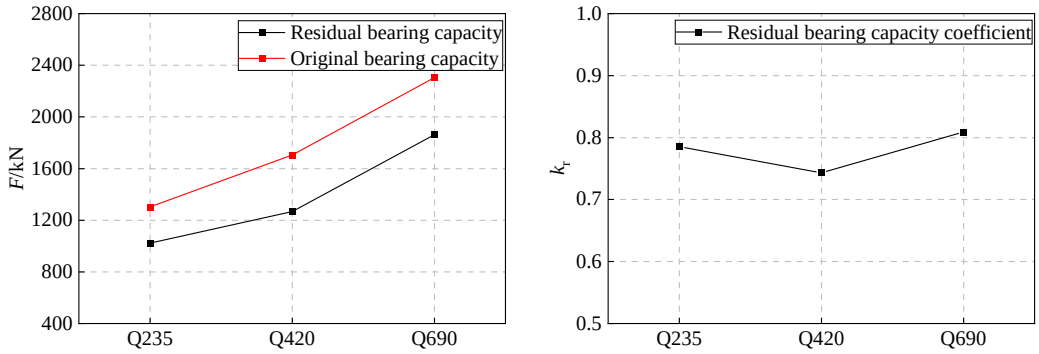

Figure 2: Influence of steel strength

3.2.2 Concrete Strength

While keeping other material parameters constant, concrete strength grades C40, C60, and C80 were selected as variable parameters to analyze the residual load-bearing capacity relationship of locally corroded steel tube concrete columns after impact. As shown in Figure 3, both initial and residual load-bearing capacities gradually increase with higher concrete strength grades. For C40 concrete, the initial load-bearing capacity and residual load-bearing capacity were 1421 kN and 1184 kN respectively, with a residual load-bearing capacity coefficient kr=0.83. For C60 concrete, the initial and residual load-bearing capacities reached 1634 kN and 1268 kN respectively, with kr=0.78. When using C80 concrete, the initial and residual load-bearing capacities increased to 1856 kN and 1410 kN respectively, with kr=0.76. These results demonstrate that higher concrete strength grades progressively reduce the residual load-bearing capacity of steel tube concrete columns after impact.

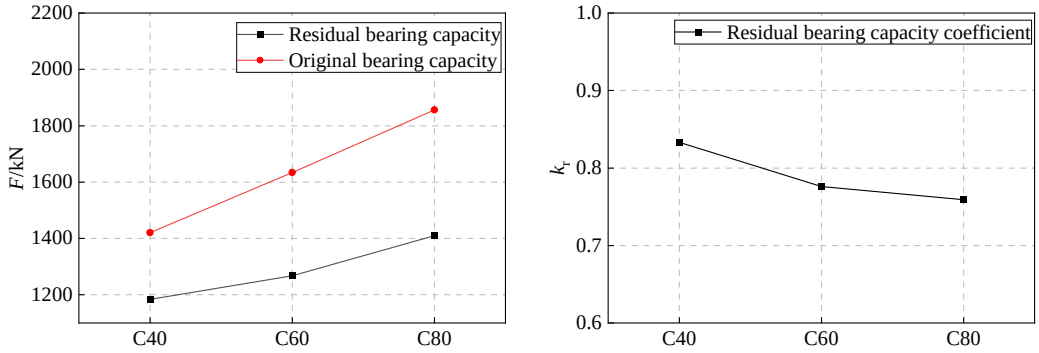

Figure 3: Influence of concrete strength grade

3.2.3 Circumferential Corrosion Angle

While keeping other material parameters constant, we selected circumferential corrosion angles of 0°,180°, and 360° as variable parameters to analyze the residual load-bearing capacity relationship of locally corroded steel-concrete composite columns after impact. As shown in Figure 4, the residual load-bearing capacity progressively decreases with increasing circumferential corrosion angles. At 0°, the original load-bearing capacity and residual load-bearing capacity were 1706 kN and 1486 kN respectively, with a residual load-bearing capacity coefficient kr=0.87. At 180°, the original and residual load-bearing capacities decreased to 1706 kN and 1268 kN respectively, with kr=0.74. At 360°, the original and residual load-bearing capacities further declined to 1706 kN and 904 kN

respectively, with kr=0.53. These results demonstrate that the residual load-bearing capacity of steel-concrete composite columns post-impact weakens significantly with increasing circumferential corrosion angles.

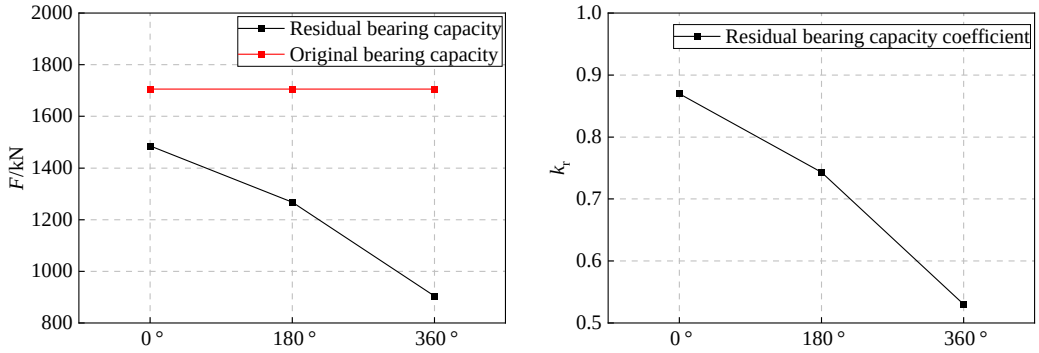

Figure 4: Influence of circumferential corrosion angle

3.2.4 Axial Corrosion Length Ratio

While keeping other material parameters constant, we selected three axial corrosion length ratios (0, 1/10, and 1/3) relative to specimen length as variable parameters to analyze the residual load-bearing capacity relationship of impact-affected steel-concrete composite columns with localized corrosion. Figure 5 demonstrates that residual load-bearing capacity decreases when transitioning from corrosion-free to corroded states, while remaining largely stable with varying corrosion defect lengths. At an axial corrosion length ratio of 0, the original and residual load-bearing capacities were 1706 kN and 1487 kN respectively, with a residual capacity coefficient kr=0.87. When the ratio increased to 1/10, both values decreased to 1706 kN and 1268 kN respectively, showing kr=0.74. At 1/3 ratio, the original and residual capacities reached 1706 kN and 1284 kN respectively, with kr=0.75. These results indicate that corrosion length ratios exhibit weakening effects on residual load-bearing capacity during impact transition from corrosion-free to corroded states. However, when corrosion zones already exist, the corrosion length ratio shows negligible impact on post-impact residual capacity.

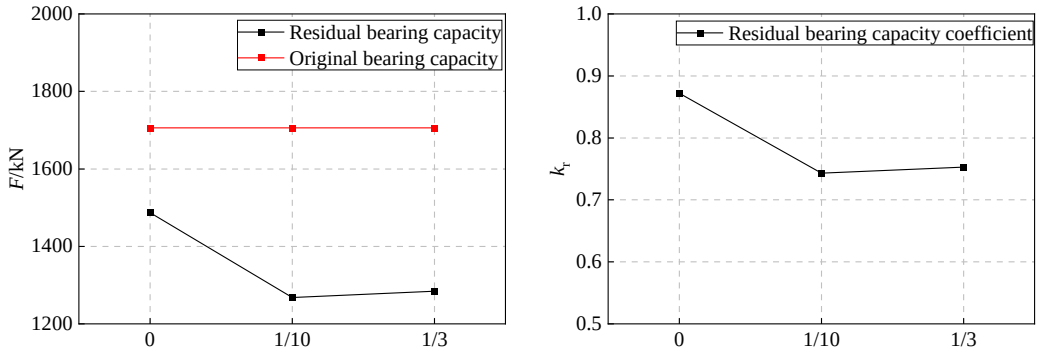

Figure 5: Effect of axial corrosion length ratio

3.2.5 Corrosion Depth Ratio

While keeping other material parameters constant, the ratio of corrosion depth to steel pipe thickness was selected as variable parameters (0, 0.5, and 1.0) to analyze the residual load-bearing

capacity relationship of locally corroded steel-concrete composite columns after impact. As shown in Figure 6, the residual load-bearing capacity gradually decreases with increasing corrosion depth ratio. When the corrosion depth ratio was 0, the original load-bearing capacity and residual load-bearing capacity were 1706 kN and 1486 kN respectively, with a residual load-bearing capacity coefficient kr=0.87. At a corrosion depth ratio of 0.5, the original and residual load-bearing capacities were 1706 kN and 1268 kN respectively, with kr=0.74. For a ratio of 1.0, the original and residual load-bearing capacities were 1706 kN and 854 kN respectively, with kr=0.50. These results demonstrate that the residual load-bearing capacity of steel-concrete composite columns after impact progressively weakens with increasing corrosion depth ratio, and the weakening effect becomes more pronounced.

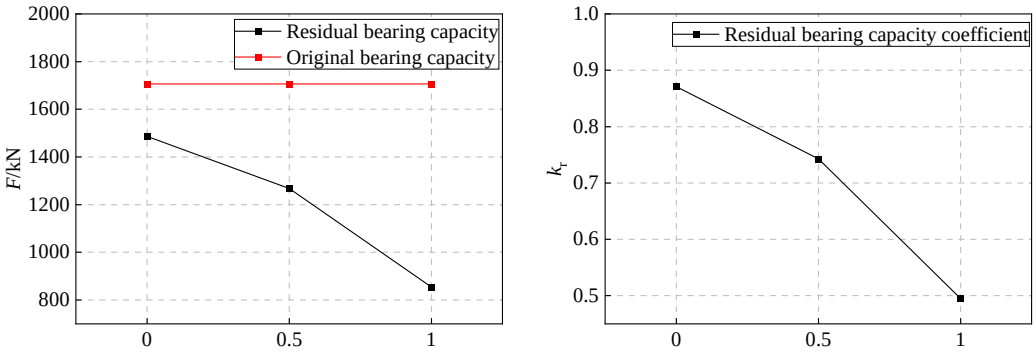

Figure 6: Effect of corrosion depth

3.2.6 Impact Energy

With other material parameters kept constant, impact energies of 4.4 kJ, 7.7 kJ, and 17.6 kJ were selected as variable parameters to analyze the residual load-bearing capacity relationship of locally corroded steel-concrete composite columns after impact. As shown in Figure 7, the residual load-bearing capacity progressively decreases with increasing impact energy. At 4.4 kJ impact energy, the original load-bearing capacity and residual load-bearing capacity were 1706 kN and 1163 kN respectively, with a residual load-bearing capacity coefficient kr=0.68. At 7.7 kJ impact energy, the original and residual load-bearing capacities were 1706 kN and 974 kN respectively, with kr=0.57. At 17.6 kJ impact energy, the original and residual load-bearing capacities were 1706 kN and 795 kN respectively, with kr=0.47. These results demonstrate that the residual load-bearing capacity of steel-concrete composite columns weakens significantly with increasing impact energy.

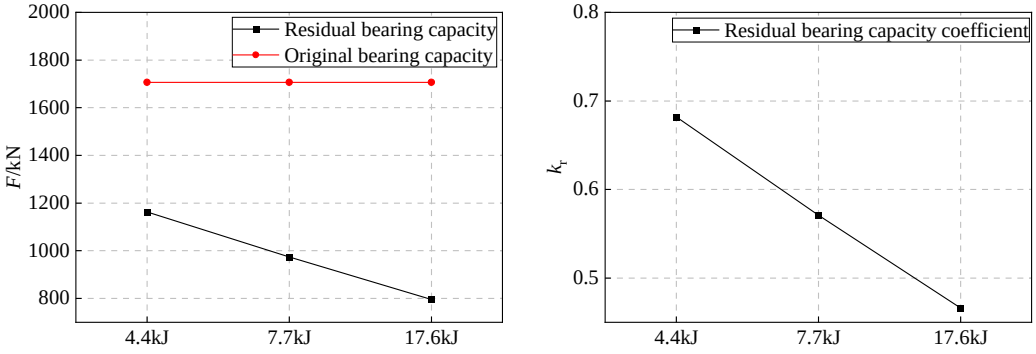

Figure 7: Effect of impact energy

4. Conclusions

This study developed an ABAQUS finite element model to analyze the residual load-bearing capacity of locally corroded circular steel tube concrete columns after impact. We investigated the effects of steel strength, concrete strength, circumferential corrosion parameters, axial corrosion length, impact energy, and corrosion depth ratio on the mechanical properties of locally corroded columns and expensive concrete columns post-impact. The analysis yielded the following conclusions:

(1) A finite element model suitable for locally corroded circular steel tube concrete columns was established, and the mechanical performance effects of the columns under impact under different operating conditions were analyzed through finite element modeling.

(2) With the increase in steel strength, the residual load-bearing capacity of locally corroded steel-concrete composite columns gradually increases; similarly, as concrete strength rises, the residual load-bearing capacity of locally corroded steel-concrete composite columns also increases.

(3) When the circumferential corrosion angle of the localized corrosion zone is altered, the larger the angle, the lower the residual load-bearing capacity of the steel-concrete composite column. Changes in axial corrosion length have no effect on its residual load-bearing capacity. Variation in corrosion depth affects the magnitude of residual load-bearing capacity, with greater corrosion depth resulting in lower residual load-bearing capacity.

(4) The greater the impact energy, the more severe the damage to the steel-concrete composite column, resulting in lower residual load-bearing capacity.

References

[1] H. Zhao, S. Mei, D.C. Wang, Wensu. Round-ended concrete-filled steel tube columns under impact loading: Test, numerical analysis and design method[J]. Thin-Walled structures, 2023, 191(Oct.): 1.1-1.17.

[2] Zhou Xiaoguang, Hou Chao, Li Wei. Corrosion damage characteristics and intelligent evaluation method for offshore steel tube concrete [J]. Journal of Architectural Structures, 2024, 45(S01):304-315.

[3] Hou Chuanchuan. Study on Mechanical Properties of Circular Steel Tube Concrete Members under Low-Speed Transverse Impact Load [D]. Tsinghua University, 2012.

[4] Lai D ,Chen Y ,Liao F , et al.UHPC-encased CFST composite columns under lateral impact: An experimental investigation[J].Journal of Constructional Steel Research,2024,222108948.DOI:10.1016/J.JCSR.2024.108948.

[5] Fu Chaojiang, Deng Shupeng, Luo Caishong, Gao Yibin. Mechanistic analysis of lateral impact on steel tube reinforced concrete columns and study on inertial forces [J]. Architectural Science, 2022, 38(9):35-45.

[6] Fu Chaojiang, Gao Ying, Chen Huayan, Luo Caishong, Wang Bizhen, Lin Youfeng, Zhang Zequn. Study on residual axial load-bearing capacity of steel tube concrete columns after lateral impact [J]. Advances in Building Steel Structures, 2024, 26(4):57-69.

[7] Wang Yifan. Remaining load-bearing capacity and damage analysis of weathering steel tube concrete columns after lateral impact [D]. Yangtze University, 2023.